

Using Waste CO₂ Generated Vaterite in Ternary Cementitious Blends

Ying Wang

Fortera Corporation
100 Great Oaks Blvd suite 120
San Jose, CA 95119, USA
ywang@forterausa.com

Craig W. Hargis

Fortera Corporation
100 Great Oaks Blvd suite 120
San Jose, CA 95119, USA
chargis@forterausa.com

Abstract – A novel process that utilizes CO₂ and reduces criteria air pollutants from cement kiln flue gas is under development. The process binds CO₂ and forms a spherical form of calcium carbonate, vaterite. Vaterite can then be blended with portland cement to produce an enhanced portland-limestone cement or with portland cement and other supplementary cementitious materials to produce ternary blended cements with lower embodied carbon. Although vaterite can be used alone as a cement, this paper will focus on using vaterite in blended hydraulic cements. The work presented introduces this new form of calcium carbonate, and the cementitious materials formulated using vaterite. The results show that vaterite can be used to produce blended cements that have superior properties than blended cements without vaterite, while avoiding additional milling time, which can increase plant capacity when milling operations are a constraint. Blended cements can be produced utilizing vaterite that have low carbon footprints, good durability performance, improved early-age strengths, the required ultimate strengths, faster setting times, and good workability. Manufacturing this new cementitious material can help cement producers achieve their sustainability goals.

Index Terms – cement industry, carbon emissions, mortar, concrete, materials

I. INTRODUCTION

As the largest manufactured product in the world, cement production plays a substantial role in anthropogenic CO₂ emissions, contributing to approximately 7-8% of these emissions, as well as consuming over 3% of the global energy demand and emitting over 5% of global anthropogenic PM₁₀ emissions [1,2]. Given the ongoing global trends of population growth and urbanization, these environmental impacts are expected to persist unless mitigation strategies are implemented. In recent years, various technical measures have emerged to mitigate these impacts. For instance, the waste CO₂ from cement kilns and fossil fuel incinerators can be harnessed through processes such as carbonation curing, secondary chemical reactions for carbon capture [2,3], or geological storage [4]. However, these measures frequently encounter technical and economic challenges when applied in cement plants, especially in developing countries where most cement will be produced and used [2].

Adoption of blended cements, such as portland-limestone cement, portland-pozzolan cement containing fly ash, natural pozzolan, or calcined clay, and ternary blended cement containing pozzolan, slag, or calcium carbonate, has increased over recent decades [5,6]. These blended cements can offer additional hydration or pozzolanic reactions, often resulting in improved properties at various stages of curing [5–9]. This approach can significantly reduce CO₂ emissions in the cement industry by minimizing the quantity of clinker required by incorporating supplementary cementitious materials (SCMs) or fillers into blended cement formulations with optimized mix designs [2,4]. However, the use of SCMs in blended cement can also introduce challenges. For example, calcined clay can lead to increased water demand in blended cements, necessitating the use of superplasticizers, which may escalate production costs [10–12]. Furthermore, the inclusion of fly ash can prolong setting times and reduce early-age strength [13]. Although certain types of SCMs bring drawbacks in blended cements, effective formulation of blended cements can address some of these issues economically [14,15].

Limestone, primarily composed of calcium carbonate (CaCO₃), has traditionally been employed in the cement industry. Portland cement often contains up to 5% calcium carbonate, while portland-limestone cement may contain up to 15-35% calcium carbonate, depending on the region. The addition or co-grinding of calcium carbonate in cement not only provides additional nucleation sites for C-S-H formation but also contributes to the clinker phases' hydration reactions [5,6,8]. The physical nucleation effect, particles shearing effect [16], and improved packing brought about by calcium carbonate additions accelerate cement hydration. Additionally, the reaction between calcium carbonate and aluminates yields carboaluminates as supplementary hydration products, enhancing cement strength and durability [6,17]. The interaction between reactive aluminates and carbonate ions makes fine calcium carbonate a potential candidate in blended cements to co-substitute for clinker with aluminosilicate-based SCMs, such as slag, fly ash, and calcined clay [18].

Calcite constitutes the primary mineral phase in limestone, alongside the less common anhydrous polymorphs of calcium carbonate, aragonite, and vaterite. Vaterite, albeit less stable and more soluble, can be generated from CO₂ from cement kilns. It

exhibits cementitious properties when mixed with water and can be used as a supplementary material in blended cements. Vaterite, with its higher specific surface area, solubility, and dispersion compared to calcite and aragonite, is frequently employed in the food industry and biomedical applications [19]. Various synthesis methods, including CO₂ bubbling, reverse emulsion, and solution precipitation, have been utilized to produce vaterite [20]. Researchers have successfully generated vaterite using different approaches [19,21,22]. As a potential construction material, vaterite-based cement paste has been shown to attain an ultimate strength of 40 MPa after 3 days of curing at 80°C [22]. In addition to its independent cementitious properties [22,23], vaterite can serve as a supplementary material for blended cements [24–26]. Studies have demonstrated that cement paste incorporating vaterite exhibits lower porosity compared to calcite or aragonite, owing to the higher solid volume formed with vaterite inclusion [27]. Furthermore, vaterite has been utilized as an internal curing agent due to its porous structure [20], leading to reduced autogenous shrinkage in mixtures containing vaterite [27–29].

The optimal utilization of SCMs in blended cement has the potential to reduce CO₂ emissions by approximately 44% in the cement industry [1], and this measure is supported by various standards organizations, including ASTM and AASHTO in the United States, and CEN in Europe. Nevertheless, the availability of some SCMs, such as fly ash and slag, is diminishing due to the closure of coal-fired power plants and changes to the steel manufacturing processes globally, prompting the exploration of alternative materials for blending with cement [13,30].

This paper delves into the utilization of vaterite in blended cements and presents the outcomes and advantages of incorporating 5-10% vaterite as a replacement for SCMs in two ternary blended cement formulations. This study encompasses various characterization techniques, including isothermal calorimetry and thermogravimetric analysis, to investigate the hydration of blended cement pastes, with and without the inclusion of vaterite. Fresh properties such as mortar flow and setting time, as well as hardened properties like mortar compressive strength, bulk resistivity, and durability, were examined at different curing ages and compared between cement blends containing 5-10% vaterite and their non-vaterite counterparts.

II. MATERIALS AND METHODS

A. Materials

In this study, ASTM C150 Type II-V cement, ASTM C618 low calcium fly ash, ASTM C989 slag, and lab-synthesized vaterite were employed. The synthesis process for vaterite has been previously documented [22,31,32]. The vaterite utilized in this study consisted of 97.1% vaterite and 2.9% calcite. Fig. 1 illustrates the morphology of vaterite particles as observed under scanning electron microscopy (SEM). These vaterite particles display a spherical shape with a textured surface and are comprised of agglomerations of numerous microplates and lenses that form a rosette-like mesostructure.

The median particle size (d_{50}) of the raw materials was determined using a laser particle size analyzer. A thermogravimetric analyzer (TGA) was employed to assess the loss on ignition (LOI) of the raw materials. For the particle size distribution (PSD) measurements of cement in isopropyl alcohol (IPA), a refractive index of 1.7 was applied, while a refractive index of 1.58 was used for vaterite in water. The density of the raw materials was examined using a gas pycnometer, and the specific surface area of the raw materials was determined through analysis with a physisorption analyzer. The major mineral phases of raw materials were determined by an X-ray powder diffraction analyzer. Detailed characterization results are presented in Table 1.

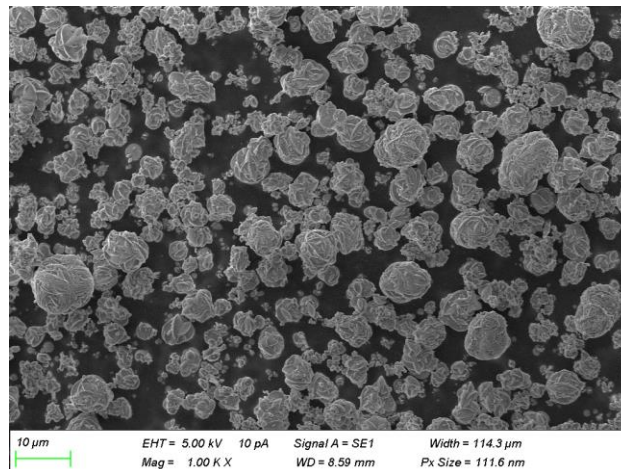


Fig.1. SEM image of the vaterite particles.

Table 1. Mineral phase compositions (%), LOI (%), d50 values (μm), density (g/cm^3) and surface area (m^2/g) of the raw materials.

Material	d ₅₀	Density	Surface area	LOI	Major mineral phases determined by XRD
Cement	12.7	3.2	1.3	1.7	Alite (62.3), Belite (12.0), Ferrite (11.2), Aluminate (5.1)
Fly ash	23.3	2.1	2.3	0.6	Amorphous (66.3), Mullite (23.5), Quartz (9.5)
Slag	6.3	3.0	1.5	1.4	Amorphous (78.9), Alite (11.0), Anhydrite (7.1), Hatrurite (3.0)
Vaterite	5.7	2.5	5.5	43.5	Vaterite (97.1), Calcite (2.9)

B. Mixture Design

To assess the influence of SCMs and vaterite, these materials were employed to partially replace 25–30% of the cement in the mixtures by mass. Analysis of the hydration process was conducted on paste samples using isothermal calorimetry and thermogravimetric analysis (TGA). Pastes for hydration analysis were formulated according to Table 2 with a fixed water-to-binder ratio (w/b) of 0.6.

To assess the hardened properties of the materials, including compressive strength and bulk resistivity, mortar cubes were prepared in accordance with the ASTM C109 standard. Durability tests were carried out on mortar bars to evaluate resistance to sulfate attack and alkali-silica reaction (ASR). All mortar cubes and mortar bars used in the ASTM C1012 sulfate resistance tests were formulated according to Table 3. Mortar bars utilized in the ASTM C1567 accelerated mortar bar test (AMBT) were formulated according to Table 4.

Table 2. Mixture designs of cementitious pastes for hydration analysis given for 100 g of binder (w/b = 0.6).

Mixture	Cement (g)	Fly ash (g)	Slag (g)	Vaterite (g)	Water (g)
75C_25F	75	25	0	0	60.0
75C_15F_10V	75	15	0	10	60.0
70C_30S	70	0	30	0	60.0
70C_20S_10V	70	0	20	10	60.0

Table 3. Mixture designs of all mortar cubes and ASTM 1012 mortar bars given for 100 g of binder (w/b = 0.485, s/b = 2.75).

Mixture	Cement (g)	Fly ash (g)	Slag (g)	Vaterite (g)	Sand (g)	Water (g)	Flow (%)
75C_25F	75	25	0	0	275	48.5	115
75C_20F_5V	75	20	0	5	275	48.5	118
75C_15F_10V	75	15	0	10	275	48.5	116
70C_30S	70	0	30	0	275	48.5	106
70C_25S_5V	70	0	25	5	275	48.5	105
70C_20S_10V	70	0	20	10	275	48.5	115

Table 4. Mixture designs of mortar bars in ASTM 1567 accelerated mortar bar test given for 100 g of binder (w/b = 0.47, s/b = 1.90).

Mixture	Cement (g)	Fly ash (g)	Slag (g)	Vaterite (g)	Reactive aggregate (g)	Water (g)
75C_25F	75	25	0	0	190	47
75C_15F_10V	75	15	0	10	190	47
70C_30S	70	0	30	0	190	47
70C_20S_10V	70	0	20	10	190	47

C. Methods

1) Isothermal Calorimetry

An isothermal calorimeter was employed to evaluate the heat of hydration in cementitious paste mixtures. Initially, 20 grams of dry powder were manually mixed for 2 minutes in a beaker, after which 12 grams of deionized water were added. The resulting pastes underwent an additional 2 minutes of manual mixing in the same beaker. Approximately 10 grams of the paste were then transferred to glass ampoules. Once all 8 samples were securely sealed in the ampoules, they were placed in the isothermal calorimeter, which had been pre-conditioned to 23 ± 0.05 °C. The entire paste mixing process was completed in under 20 minutes.

for all 8 samples. Heat release was monitored in the calorimeter over 7 days and normalized to the binder mass. Triplicate tests on one sample demonstrated a heat of hydration test coefficient of variation (CoV) of less than 3%.

2) *Thermogravimetric Analysis*

Cementitious pastes were employed for hydration products analysis using a thermogravimetric analyzer. Approximately 70 grams of fresh paste were prepared as detailed previously, which was subsequently loaded into three cylindrical vials, each with a capacity of 10 ml. These vials, once sealed, were affixed to a vertically rotating cylinder, operating at a rotational speed of 20 rpm for a duration of 7 hours, with the aim of mitigating material and water separation prior to their relocation to a controlled environment set at 23°C. Hydration was stopped at intervals of 7, 28, and 56 days. The paste was crushed and immersed in IPA to facilitate solvent exchange, effectively halting the hydration process. For TGA analysis, a quantity ranging from 30 to 50 milligrams of the paste was loaded into the TGA crucible and subjected to a preliminary drying process at 40°C for a period of 20 minutes before the initiation of the heating cycle. The temperature was then incrementally raised at a rate of 10°C per minute, ranging from 40°C to 900°C, all while maintaining an inert N₂ atmosphere. The quantification of the mixtures' hydration products was based on the measurement of mass losses occurring at specific temperature intervals, utilizing the tangential methodology elucidated by Kim and Olek [33]. In the 150-600°C temperature range, the mass loss on the TGA curve indicated the bound water content of the paste [34]. Furthermore, the water loss from Ca(OH)₂ was denoted by the mass loss between 380-460°C [33,35]. The release of CO₂ from CaCO₃ decomposition was signified by the mass loss within the 600-900°C range [33,35]. It is important to note that the decomposition of carboaluminates resulted in some mass loss at a lower temperature range [35]. Based on their corresponding weight loss values, the content of these hydration products can be calculated. The TGA tests exhibited a CoV of less than 2% in triplicate testing on a single sample.

3) *Setting Time*

The determination of setting time for the mixtures followed the guidelines specified in ASTM C191. To achieve the desired normal consistency, trials were conducted by mixing 650 grams of the binder with varying amounts of water. Subsequently, the paste with normal consistency was placed into a conical ring, and the setting time was measured using an automatic Vicat machine.

4) *Compressive Strength & Mortar Flow*

Mortar preparations were carried out as outlined in ASTM C305, with subsequent casting into 50 mm mortar cubes in accordance with ASTM C109. Prior to mixing, the binders underwent homogenization using a powder blender. A consistent water-to-binder ratio (w/b) of 0.485 was employed for all mixtures. Mortar flow measurements were performed following ASTM C1437 guidelines. In each case, a total of 12 mortar cubes were fabricated, with testing conducted on 2 cubes at the ages of 1, 3, and 7 days, and 3 cubes tested at 28 and 56 days. Mortar cubes were stored in a saturated lime bath at 23°C until testing. The reported results are based on the average values, and the CoV for the compressive strengths remained below 5% at all specified ages.

5) *Bulk Resistivity*

Measurements of bulk resistivity for the mixtures were conducted on the mortar cubes prior to compressive strength evaluations. The Giatec RCON resistivity meter was employed to assess the 50 mm mortar cubes following the guidelines of ASTM C1876. These measurements were performed on surface-dry specimens at a frequency of 1 kHz. Corrections for the geometric dimensions of the cube specimens were applied to the obtained data, and the resulting average value across all tested cubes is presented. The CoV for the measurements remained consistently below 6% throughout all stages of the study.

6) *Accelerated Mortar-Bar Test for Alkali Silica Reaction (AMBT)*

Mortar bars, equipped with gauge studs at both ends, were fabricated and assessed in accordance with ASTM C305 and ASTM C1567. Graded borosilicate glass was prepared as the reactive aggregate in accordance with the grading requirements specified in ASTM C1567. For each mixture, a set of three bars was cast. The water-to-binder ratio (w/b) and the sand-to-binder ratio (s/b) were consistently maintained at 0.47 and 1.90, respectively, for all AMBT mortar bars in the study. After casting, the bars underwent an initial 1-day curing period in a controlled moist environment at 23°C before demolding. Subsequently, they were transferred to an 80 ± 2°C water bath. Following 24 hours in the 80°C water bath, the bars were measured for their zero comparator readings. The bars were then immersed in a 1 M NaOH solution at 80 ± 2°C, and subsequent comparator readings were recorded. In accordance with ASTM C1567, any expansion exceeding 0.1% of the nominal gauge length after 14 days in the NaOH solution would signify potential deleterious expansion attributed to alkali-silica reaction (ASR). The reported

expansion values represent the average among the three bars within a given mixture, with the CoV for expansion measurements consistently remained below 2% across all mixtures.

7) Sulfate Exposure Resistance Test

The sulfate exposure test was conducted in accordance with ASTM C1012. The mortar bars were prepared with a consistent water-to-binder ratio (w/b) of 0.485 and sand-to-binder ratio (s/b) of 2.75. The ASTM C778 graded standard sand was used in this test. Following the test procedure, six mortar bars and cubes were prepared following the guidelines of ASTM C305. Upon achieving an average strength of 20 MPa for two of the cubes within the same mixture, the initial lengths of the bars were measured. Subsequently, these bars were immersed in a 5% Na_2SO_4 solution and stored in a controlled moist environment at $23 \pm 2^\circ\text{C}$. Periodic measurements were taken, and at each measurement occasion the sodium sulfate solution was replaced. The reported expansion values reflect the average among the six bars in a specific mixture, with the CoV for the expansion measurements consistently remaining below 2% across all mixtures.

III. RESULTS AND DISCUSSION

A. Heat of Hydration

Fig. 2 illustrates the heat flow and heat release during the hydration of pastes, comparing those with and without the incorporation of vaterite. Specifically, the 25% fly ash binary paste, 75C_25F, exhibited its peak heat flow at approximately 11.7 hours following the initial mixing. Upon substituting 10% of the fly ash with vaterite, a notable shift was observed, with the peak heat flow occurring at approximately 10.8 hours and registering a higher intensity. The most pronounced peak in heat flow was primarily attributed to the hydration of C_3S , while the subsequent shoulder peak, occurring at a later stage, was a result of the C_3A reaction. The introduction of 10% vaterite as a substitute for fly ash effectively enhanced the C_3A reaction within the cementitious paste, evident in the earlier occurrence of the C_3A reaction shoulder peak as compared to the paste without vaterite. This phenomenon was also observed in the slag-vaterite mixtures, where the aluminate hydration peak was expedited.

The presence of vaterite was anticipated to accelerate C_3A reactions, owing to its superior reactivity in comparison to calcite or limestone. Vaterite can engage in more rapid interactions with aluminates during the early stages of hydration, resulting in the formation of carboaluminates while consuming C_3A and monosulfate, which also stabilizes ettringite [5,11,24,36]. Moreover, the additional aluminates introduced into the system by fly ash and slag during their pozzolanic reaction and hydration processes further accelerated the vaterite reaction. The synergistic effects from the interaction between vaterite and aluminosilicate-based SCMs have the potential to yield enhanced mechanical properties over time [18,37,38].

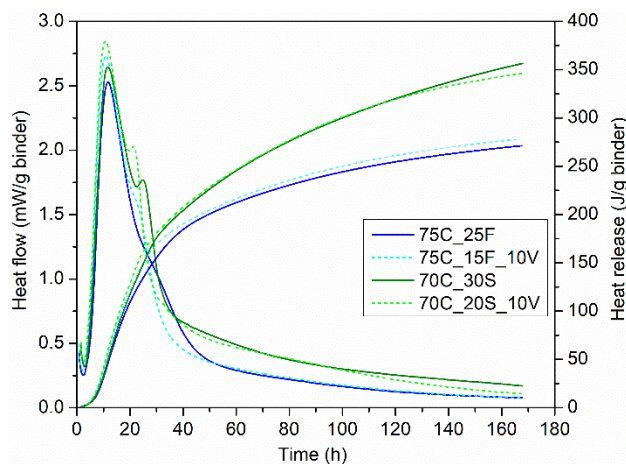


Fig. 2. Heat flow and cumulative heat release of cementitious pastes with and without vaterite.

B. Thermogravimetric Analysis

Fig. 3 presents the TGA results of the cementitious pastes with and without vaterite in fly ash and slag systems. The TGA mass loss curves quantified hydration by measuring the contents of $\text{Ca}(\text{OH})_2$ and bound water. In the hydration analysis, the paste mixtures without vaterite were compared to their counterparts containing 10% vaterite. Phase content calculations were

standardized to the weight of the heated sample or the anhydrous binder at 600°C [39]. Between 7 and 56 days in all systems, the remaining CaCO_3 in the paste is reduced by up to 1% due to vaterite's interaction with the reactive alumina. In the cement-fly ash-vaterite system, replacing fly ash with 10% vaterite produced more Ca(OH)_2 and bound water contents at 7 days, indicating enhanced early-age hydration. This outcome aligns with expectations, as the finer particle size vaterite ($d_{50} = 5.7 \mu\text{m}$) replaced the coarser fly ash powder ($d_{50} = 23.3 \mu\text{m}$), and the early-stage hydration was significantly accelerated by the nucleation of C-S-H on the surface of vaterite. Fly ash, being a material that reacts more slowly, typically provides limited hydration benefits to blended cements during early-ages. Vaterite, as a less stable polymorph of calcium carbonate, may offer a greater supply of carbonate ions for reacting with the reactive alumina. This promotes the early-stage hydration of blended cements and facilitates the dissolution of reactive alumina from fly ash particles. However, the improvements on hydration products became less prominent at 28 and 56 days, as the fly ash pozzolanic reaction proceeded.

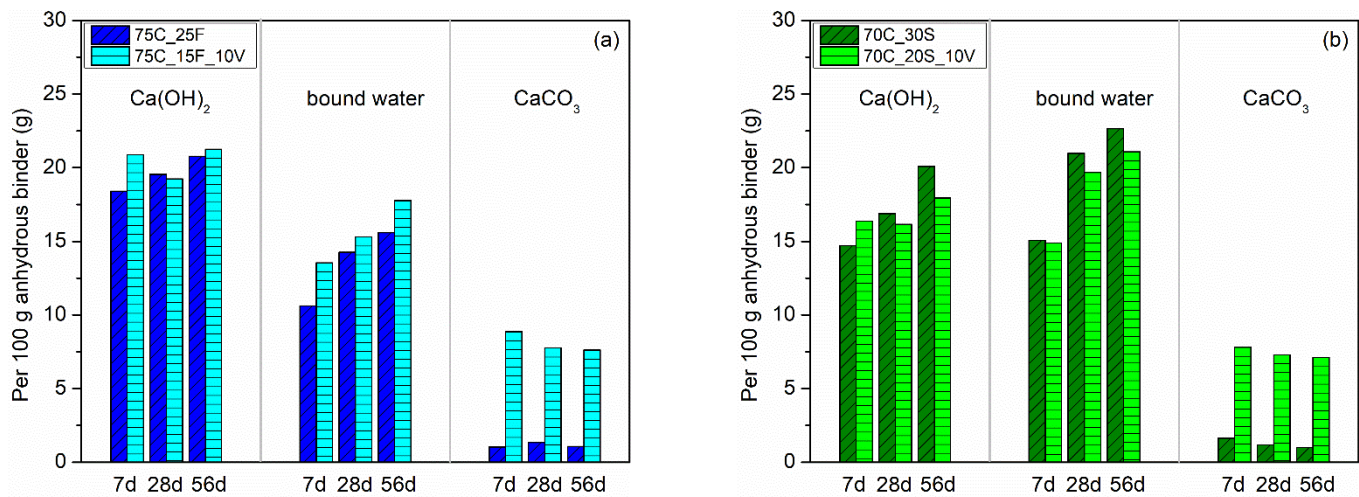


Fig. 3. Thermogravimetric analysis of cement pastes hydration products for the a) cement-fly ash-vaterite and b) cement-slag-vaterite systems.

In the cement-slag-vaterite systems, the use of 10% vaterite to replace slag did not lead to as a significant enhancement in hydration as in the fly ash system. This was expected since vaterite was replacing a very fine ($d_{50} = 6.3 \mu\text{m}$) and reactive component of slag in the blend. Notably, the total bound water content of the 70C_20S_10V mixture remained similar to or slightly less than the 70C_30S mixture at all ages. This suggests that the 10% vaterite replacement achieved hydration benefits on par with slag itself, although through a different mechanism. The interaction between vaterite, slag, and cement facilitated a reduction in slag content while maintaining similar levels of hydration products over the course of 56 days.

For specific cement compositions, the correlation between bound water content of hydrated cement pastes and the strength of the corresponding mortars or pastes has been widely observed in literature at various stages [40,41]. Therefore, an increase of the bound water content within specific cement blends is expected to enhance both the total hydration product volume and compressive strength. This study also demonstrated a positive and linear connection between the pastes' bound water contents and the corresponding mortar strengths, as depicted in Fig. 4. The inclusion of 10% vaterite in place of fly ash in various systems resulted in an approximate 20% increase in the bound water content, indicating a corresponding 20% elevation in the overall hydration degree. When replacing slag, the introduction of 10% vaterite did not compromise the overall hydration degree. The merits of vaterite encompass physical influences, such as particle shearing, an increased water-to-clinker ratio, greater nucleation of C-S-H on the vaterite surface, and a chemical reaction occurring between vaterite and aluminates. These benefits are complementary to the benefits of SCMs in blended cements.

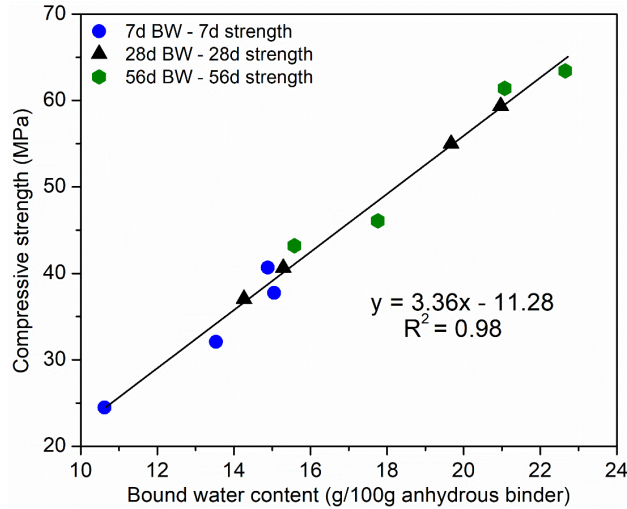


Fig. 4. The correlations between cementitious pastes' 7-, 28-, and 56-day bound water content (BW) and the corresponding mortars' 7-, 28-, and 56-day compressive strength.

C. Setting Time

In Fig. 5, a comparison of initial setting times between cement pastes with and without vaterite is presented. In the cement-fly ash-vaterite and cement-slag-vaterite systems, the incorporation of 10% vaterite led to a reduction in the initial setting time by 18 and 19 minutes, respectively. The addition of vaterite as a substitute for fly ash and slag resulted in a shorter initial setting time. The difference in setting time between vaterite-containing and vaterite-free mixes consistently aligned with the time at which peak heat flow was observed in calorimetry tests. A faster time to reach peak heat flow indicates an accelerated hydration reaction, attributed to the increased surface area available for the growth of C-S-H, as supported by the TGA results. With a greater specific surface area, vaterite particles offer more nucleation sites during the early stages of hydration compared to other SCMs or cement particles, ultimately enhancing the gel-space ratio within the hydration matrix structure and leading to higher compressive strengths [18]. Additionally, vaterite exhibits higher reactivity relative to other calcium carbonate polymorphs. The presence of dissolved carbonate ions from vaterite contributes to a higher degree of reaction with aluminates, thereby promoting an overall increase in the degree of hydration of the mixtures. This, in turn, leads to the formation of more hydration products that enhance the strength of the final blended cements [24,27].

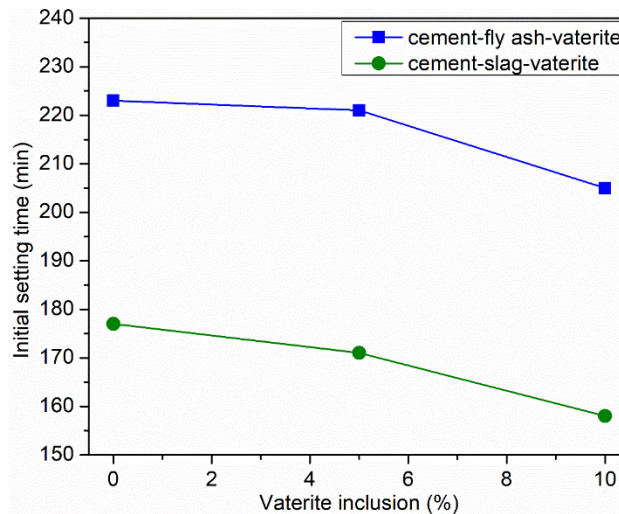


Fig. 5. The initial setting time of cementitious pastes with and without vaterite in two ternary systems.

D. Mortar Flow and Compressive Strength

Fig. 6 presents a comparison of compressive strength development in the two cementitious systems, featuring varying levels of vaterite inclusions (0%, 5%, and 10%). As a key performance indicator, workability is reflected in the flow value of the mortar detailed in Table 3. The introduction of spherical vaterite, as a replacement for 10% of fly ash or slag, maintained or increased mortar flow, respectively. The replacement of 10% vaterite achieved a 9% enhancement in mortar flow in the cement-slag-vaterite system. Spherical vaterite was effective in enhancing workability, similar to fly ash.

Regarding strength development, the substitution of 5% and 10% of fly ash with vaterite led to a substantial increase of 30% to 40% in 1-day strength and a noteworthy enhancement of 19% to 31% in 7-day strength. The elevated strength observed in vaterite-incorporated mixtures persisted for a period of 56 days, demonstrating an approximate 10% increase in strength compared to the cement blend without vaterite, 75C_25F. Notably, within the cement-fly ash-vaterite system, the 10% vaterite replacement contributed more significantly at early stages, while the 5% replacement exhibited a more pronounced strength increase at later ages.

Nonetheless, achieving similar enhancement effects to fly ash replacement might not be as straightforward when substituting a faster-reacting component, such as fine slag. In the cement-slag-vaterite system, either a 5 or 10% replacement of slag with vaterite increased the mortar strength through 7 days. The most substantial strength improvement occurred at 3 days with approximately a 20% increase. The 1- and 7-day strengths were increased by approximately 10%. At 28 and 56 days, 5-10% vaterite replacement exhibited a reduction in strength of approximately 10 and 5%, respectively, compared to the slag-cement binary mixture. The diminished enhancement of hydration over time in the slag ternary system aligns with the findings from calorimetry and TGA analysis.

In both ternary systems, the most substantial early-age strength enhancement was observed when incorporating a higher vaterite content (10%). The observed improvement in early-age strength aligned with the analysis of heat evolution using isothermal calorimetry. Specifically, the inclusion of 10% vaterite not only increased the peak rate of hydration but also reduced the induction time. It is well-documented that early-age strength exhibits a strong correlation with the heat of hydration [13,41–43]. A prior study also confirmed that mixtures containing vaterite displayed lower porosity and a higher solid volume in the cement paste compared to their aragonite or calcite counterparts [27]. At later ages till 56 days, vaterite replacements of 5-10% in both systems yielded compressive strength ranging from 90 to 119% of the control blended cements without vaterite.

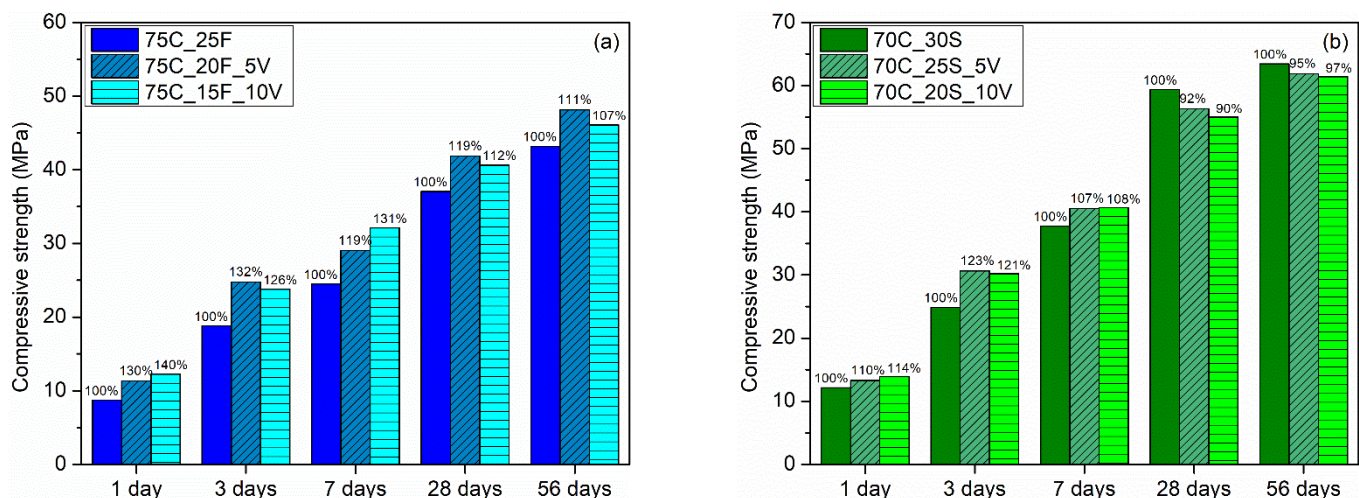


Fig. 6. The strength development of blended cement mortars for the a) cement-fly ash-vaterite and b) cement-slag-vaterite systems.

E. Bulk Resistivity

The penetration of fluids and the infiltration of aggressive ions, such as Cl^- , alkali, and SO_4^{2-} , can be rapidly assessed through electrical resistivity or conductivity. Bulk electrical resistivity, which relies on the pore structure, composition of the pore solution, specimen saturation, and temperature, serves as a key material property. Within a given set of binder constituents, a higher value of bulk resistivity typically signifies a material's higher durability and its enhanced resistance to the intrusion of ions. Fig. 7 illustrates the varying degrees of enhancement in the bulk resistivities of all systems due to the incorporation of vaterite. In the cement-fly ash-vaterite system, replacing 5% of fly ash with vaterite led to a 19% increase in bulk resistivity at 56 days. Within the cement-slag-vaterite systems, the inclusion of 5% vaterite significantly raised the bulk resistivity by 41% at 56 days.

In the previous tests, vaterite's presence was shown to increase the hydration of the binder. This enhancement in the degree of reaction of blended cements was driven by the higher surface area [18,38]. Additionally, dissolved carbonate ions interacted with the reactive alumina present in the SCMs [10,24,27,44], leading to the gradual generation of extra hydration products. Over time, ion mobility was hindered and ion absorption was encouraged by this well-structured pore system and the presence of supplementary hydration products like interlayer structured carboaluminates [45]. These effects, collectively, contributed to an improvement in the electrical resistivity of the sample. The inclusion of vaterite and SCMs likely promoted both pore refinement and a decrease in the alkalinity of the pore solution, and resulted in a reduced mass transport within the sample, ultimately boosting its electrical resistivity [8].

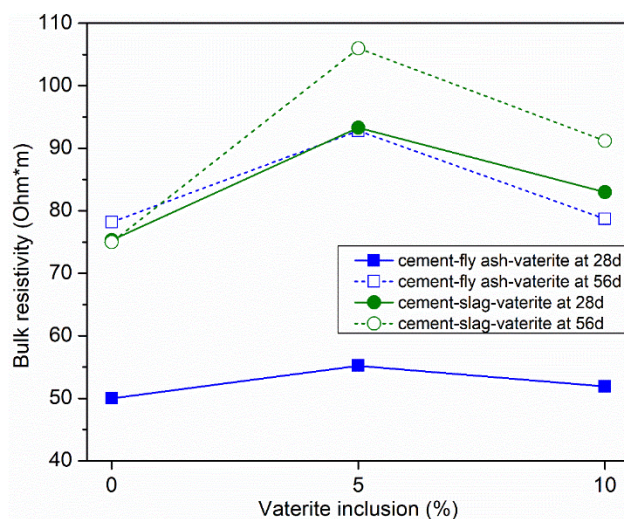


Fig. 7. Bulk resistivity development of blended cement mortars with and without vaterite.

F. AMBT Expansion

As illustrated in Fig. 8, the AMBT expansion of mortar bars subjected to an 80°C alkaline solution for 10 weeks was evaluated. According to ASTM standard C1567, an expansion of less than 0.10% within the initial 14 days (equivalent to 16 days post-casting) suggests the resulting expansions in concrete are likely to meet acceptable standards, and more importantly, a reduced risk of deleterious ASR expansion in real-world field conditions. In this study, the testing period was prolonged for further evaluation, and the results indicate that expansion remained well below 0.10% for 10 weeks for mortars with and without vaterite in both the fly ash and slag systems. These results correspond with the findings from the bulk resistivity tests and suggest that the mixtures containing vaterite sustained their durability characteristics through later ages of testing. These findings provide strong support for the efficacy of vaterite as a viable material for enhancing blended cements.

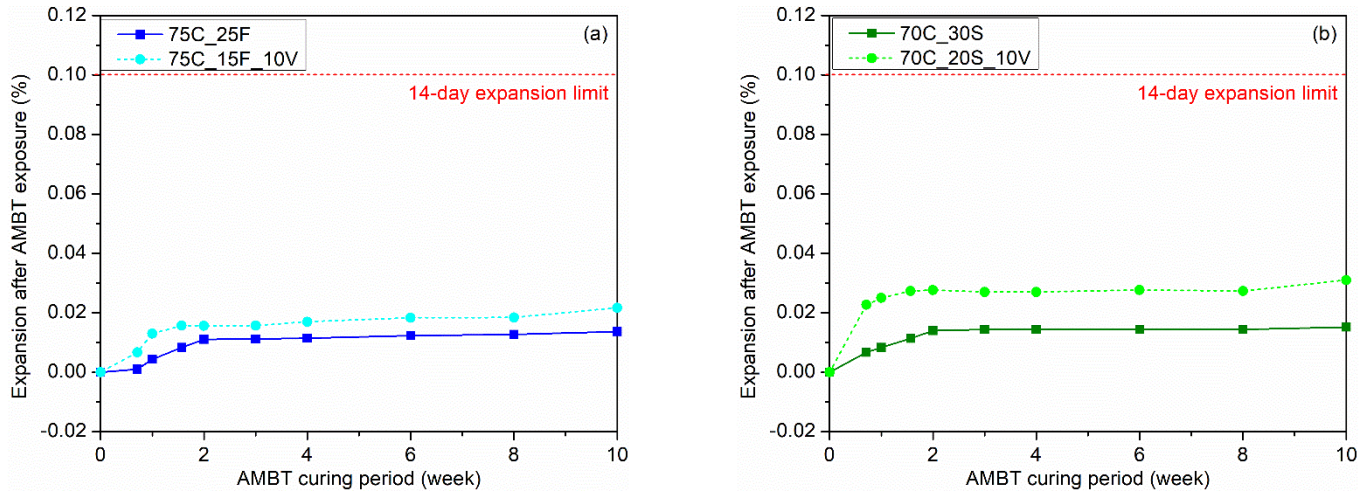


Fig. 8. The AMBT expansion of mortar bars for the a) cement-fly ash-vaterite and b) cement-slag-vaterite systems.

G. Sulfate Exposure Expansion

In Fig. 9, the expansion of mortar bars following exposure to sulfate conditions over a two-month period is presented, with ongoing testing currently in progress. To meet the criteria for classification as high sulfate resistant cement under the testing protocol in ASTM C1012, it is required that the 6-month expansion limit does not exceed 0.05%, or the 1-year expansion limit remains below 0.10%. During the testing phase in both systems, the expansion of mortar bars containing vaterite was similar to that of their non-vaterite counterparts, but slightly higher by 8 weeks. Expansion due to chemical sulfate attack in concrete is attributed to the formation of secondary minerals that exert pressure on the hardened cement paste. Early stages of the reaction are often associated with the formation of ettringite, a process contingent upon the presence of two critical constituents, unhydrated calcium aluminate and monosulfoaluminate. The inclusion of vaterite diminishes the risk of secondary ettringite formation, resulting in reduced expansion when the mortar bars are exposed to sulfate solutions. The incorporation of vaterite in the cement matrix initiates a reaction where the calcium aluminate component interacts with carbonate ions, leading to the formation of stable carboaluminates. This chemical transformation effectively stabilizes the ettringite within the mixture, preventing its conversion into monosulfoaluminate and then into secondary ettringite. A denser cement paste matrix with a reduction in pore connectivity can also be achieved by vaterite inclusion.

In the two-month testing period, the inclusion of 10% vaterite to replace fly ash or slag produced expansion levels similar to their non-vaterite counterparts, consistent with their performance in bulk resistivity measurements. Testing is ongoing to see if the amount of fly ash and slag included is sufficient to densify the microstructure enough to limit ion mobility and to stifle slower sulfate attack reactions such as the formation of gypsum from calcium in the pore solution, which is mostly from calcium hydroxide and to a lesser extent from C-S-H. The amounts of SCM used in this study are below the amounts generally used to control sulfate attack and additional SCM would likely be prescribed in exposure conditions with sulfate present.

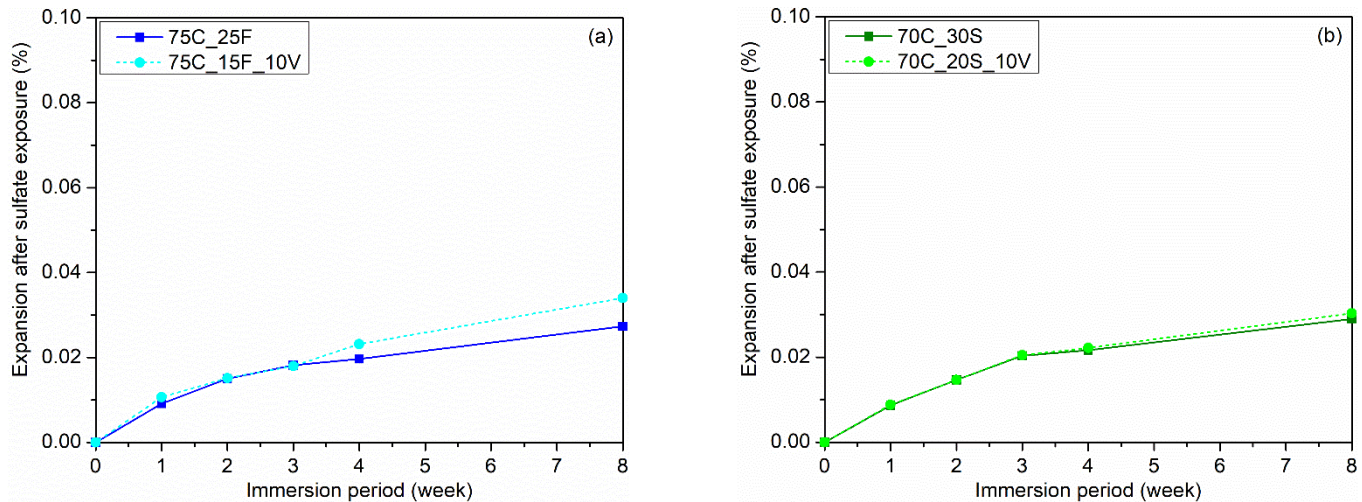


Fig. 9. The expansion of mortar bars for the a) cement-fly ash-vaterite and b) cement-slag-vaterite systems.

IV. CONCLUSIONS

This paper presents findings and advantages of substituting SCMs in two blended cements with vaterite at levels between 5% and 10%. In the cement-fly ash blends, the replacement of 10% of fly ash with vaterite resulted in a 40% increase in strength after 1 day, and the increased compressive strength persisted over a 56-day period when compared to the control cement-fly ash blend. For the cement-slag blends, a 10% replacement of slag with vaterite led to approximately a 20% increase in strength at 3 days. A 10% addition of vaterite also reduced the initial setting time of both fly ash and slag blended cements by approximately 20 minutes. Moreover, an enhanced bulk resistivity at later stages was also achieved by vaterite inclusion, indicating the potential for vaterite-containing blended cements that offer durability as well. This was corroborated by the alkali-silica reaction (ASR) test results and the initial sulfate attack results, which indicate the ability to formulate durable blended cements that incorporate vaterite. Hydration analysis, employing isothermal calorimetry and thermogravimetry, verified the acceleration of early-age hydration reactions due to the physical and chemical properties of vaterite. The presence of vaterite expedited both major hydration peaks of silicates and aluminates. Furthermore, the total heat release of the paste containing vaterite and fly ash exceeded its counterpart lacking vaterite. Given the contemporary challenges in the declining availability of traditional SCMs, vaterite exhibits the potential to extend the supply of these materials and enhance the overall performance of the resultant cement blends. This offers a viable solution to the cement and concrete industries in their pursuit of sustainability goals.

ACKNOWLEDGMENTS

The authors extend their gratitude to their project's dedicated supporters, including colleagues, scientific advisors, and investors. Special thanks are expressed to Jorge Duque, Christopher Erikson, Ryan Gilliam, Victor Gonzalez, Sarah Granke, Adriana Gutierrez, Zach Haber, Michael Kostowskyj, Keith Krugh, Claire Luethé, Jesus Gonzalez Pequeno, Manuel Rodrigues, and Aidan Svetich-Will for their invaluable contributions to material preparation and experimental work.

REFERENCES

- [1] I.H. Shah, S.A. Miller, D. Jiang, R.J. Myers, Cement substitution with secondary materials can reduce annual global CO₂ emissions by up to 1.3 gigatons, *Nat. Commun.* 13 (2022) 1–11. <https://doi.org/10.1038/s41467-022-33289-7>.
- [2] K.L. Scrivener, V.M. John, E.M. Gartner, Eco-efficient cements: Potential economically viable solutions for a low-CO₂ cement-based materials industry, *Cem. Concr. Res.* 114 (2018) 2–26. <https://doi.org/10.1016/j.cemconres.2018.03.015>.
- [3] M. Erans, S.A. Nabavi, V. Manović, Carbonation of lime-based materials under ambient conditions for direct air capture, *J. Clean. Prod.* 242 (2020). <https://doi.org/10.1016/j.jclepro.2019.118330>.
- [4] M.G. Plaza, S. Mart, F. Rubiera, Cement Industry : State of the Art and Expectations, *Energies*. (2020). www.worldcementassociation.org/images/info-graphics/001-World-Wide-Cement-Production.pdf0Awww.mdpi.com/journal/energies.

- [5] A.M. Ramezaniapour, R.D. Hooton, A study on hydration, compressive strength, and porosity of Portland-limestone cement mixes containing SCMs, *Cem. Concr. Compos.* 51 (2014) 1–13. <https://doi.org/10.1016/j.cemconcomp.2014.03.006>.
- [6] B. Lothenbach, G. Le Saout, E. Gallucci, K. Scrivener, Influence of limestone on the hydration of Portland cements, *Cem. Concr. Res.* 38 (2008) 848–860. <https://doi.org/10.1016/j.cemconres.2008.01.002>.
- [7] M.J. Tapas, L. Sofia, K. Vessalas, P. Thomas, V. Sirivivatnanon, K. Scrivener, Efficacy of SCMs to mitigate ASR in systems with higher alkali contents assessed by pore solution method, *Cem. Concr. Res.* 142 (2021) 106353. <https://doi.org/10.1016/j.cemconres.2021.106353>.
- [8] K.S.T. Chopperla, J.A. Smith, J.H. Ideker, The efficacy of portland-limestone cements with supplementary cementitious materials to prevent alkali-silica reaction, *Cement.* 8 (2022) 100031. <https://doi.org/10.1016/j.cement.2022.100031>.
- [9] K. Bharadwaj, O.B. Isgor, W.J. Weiss, Supplementary Cementitious Materials in Portland- Limestone Cements, *ACI Mater. J.* 119 (2022). <https://doi.org/10.14359/51734356>.
- [10] M.C.G. Juenger, R. Snellings, S.A. Bernal, Supplementary cementitious materials: New sources, characterization, and performance insights, *Cem. Concr. Res.* 122 (2019) 257–273. <https://doi.org/10.1016/j.cemconres.2019.05.008>.
- [11] F. Avet, K. Scrivener, Investigation of the calcined kaolinite content on the hydration of Limestone Calcined Clay Cement (LC3), *Cem. Concr. Res.* 107 (2018) 124–135. <https://doi.org/10.1016/j.cemconres.2018.02.016>.
- [12] F. Avet, X. Li, K. Scrivener, Determination of the amount of reacted metakaolin in calcined clay blends, *Cem. Concr. Res.* 106 (2018) 40–48. <https://doi.org/10.1016/j.cemconres.2018.01.009>.
- [13] Y. Wang, L. Burris, R.D. Hooton, C.R. Shearer, P. Suraneni, Effects of unconventional fly ashes on cementitious paste properties, *Cem. Concr. Compos.* 125 (2022) 104291. <https://doi.org/10.1016/j.cemconcomp.2021.104291>.
- [14] Y. Wang, P. Suraneni, Extending fly ash and pumice usage through blending with inert basaltic fines, *Mater. Struct.* 6 (2023). <https://doi.org/10.1617/s11527-023-02225-6>.
- [15] Y. Wang, S. Ramanathan, K.S.T. Chopperla, J.H. Ideker, P. Suraneni, Estimation of non-traditional supplementary cementitious materials potential to prevent alkali-silica reaction using pozzolanic reactivity and bulk resistivity, *Cem. Concr. Compos.* 133 (2022) 104723. <https://doi.org/10.1016/j.cemconcomp.2022.104723>.
- [16] E. Berodier, K. Scrivener, Understanding the filler effect on the nucleation and growth of C-S-H, *J. Am. Ceram. Soc.* 97 (2014) 3764–3773. <https://doi.org/10.1111/jace.13177>.
- [17] T. Matschei, B. Lothenbach, F.P. Glasser, The role of calcium carbonate in cement hydration, *Cem. Concr. Res.* 37 (2007) 551–558. <https://doi.org/10.1016/j.cemconres.2006.10.013>.
- [18] Y. Dhandapani, M. Santhanam, G. Kaladharan, S. Ramanathan, Towards ternary binders involving limestone additions — A review, *Cem. Concr. Res.* 143 (2021). <https://doi.org/10.1016/j.cemconres.2021.106396>.
- [19] H. Mehdizadeh, K.H. Mo, T.C. Ling, CO₂-fixing and recovery of high-purity vaterite CaCO₃ from recycled concrete fines, *Resour. Conserv. Recycl.* 188 (2023) 106695. <https://doi.org/10.1016/j.resconrec.2022.106695>.
- [20] A.M. Ferreira, A.S. Vikulina, D. Volodkin, CaCO₃ crystals as versatile carriers for controlled delivery of antimicrobials, *J. Control. Release.* 328 (2020) 470–489. <https://doi.org/10.1016/j.jconrel.2020.08.061>.
- [21] Z. Feng, T. Yang, S. Dong, T. Wu, W. Jin, Z. Wu, B. Wang, T. Liang, L. Cao, L. Yu, Industrially synthesized biosafe vaterite hollow CaCO₃ for controllable delivery of anticancer drugs, *Mater. Today Chem.* 24 (2022) 100917. <https://doi.org/10.1016/j.mtchem.2022.100917>.
- [22] C.W. Hargis, I.A. Chen, M. Devenney, M.J. Fernandez, R.J. Gilliam, R.P. Thatcher, Calcium Carbonate Cement: A Carbon Capture, Utilization, and Storage (CCUS) Technique, *Materials (Basel)*. (2021) 1–12.
- [23] J. Rodríguez-Sánchez, T. Liberto, C. Barentin, D.K. Dysthe, Mechanisms of phase transformation and creating mechanical strength in a sustainable calcium carbonate cement, *Materials (Basel)*. 13 (2020). <https://doi.org/10.3390/MA13163582>.
- [24] C.W. Hargis, A. Telesca, P.J.M. Monteiro, Calcium sulfoaluminate (Ye’elimite) hydration in the presence of gypsum, calcite, and vaterite, *Cem. Concr. Res.* 65 (2014) 15–20. <https://doi.org/10.1016/j.cemconres.2014.07.004>.
- [25] P.J.M. Monteiro, L. Clodic, F. Battocchio, W. Kanitpanyacharoen, S.R. Chae, J. Ha, H.R. Wenk, Incorporating carbon sequestration materials in civil infrastructure: A micro and nano-structural analysis, *Cem. Concr. Compos.* 40 (2013) 14–20. <https://doi.org/10.1016/j.cemconcomp.2013.03.013>.
- [26] C.W. Hargis, *Advances in Sustainable Cements*, UC Berkeley Electronic Theses and Dissertations, 2013.
- [27] D. Zhao, J.M. Williams, A.H.A. Park, S. Kawashima, Hydration of cement pastes with calcium carbonate polymorphs, *Cem. Concr. Res.* 172 (2023). <https://doi.org/10.1016/j.cemconres.2023.107214>.
- [28] O. Cherkas, T. Beuvier, F. Zontone, Y. Chushkin, L. Demoulin, A. Rousseau, A. Gibaud, On the kinetics of phase transformations of dried porous

vaterite particles immersed in deionized and tap water, *Adv. Powder Technol.* 29 (2018) 2872–2880. <https://doi.org/10.1016/j.apt.2018.08.008>.

- [29] P. Chen, J. Wang, L. Wang, Y. Xu, X. Qian, H. Ma, Producing vaterite by CO₂ sequestration in the waste solution of chemical treatment of recycled concrete aggregates, *J. Clean. Prod.* 149 (2017) 735–742. <https://doi.org/10.1016/j.jclepro.2017.02.148>.
- [30] M. Kasaniya, M.D.A. Thomas, E.G. Moffatt, Cement and Concrete Research Pozzolanic reactivity of natural pozzolans, ground glasses and coal bottom ashes and implication of their incorporation on the chloride permeability of concrete, *Cem. Concr. Res.* 139 (2021) 106259. <https://doi.org/10.1016/j.cemconres.2020.106259>.
- [31] C.W. Hargis, R.J. Gilliam, Compositions, methods, and systems to form vaterite with magnesium oxide, US 11,530,164 B2, 2022.
- [32] M. Devenney, M. Fernandez, I. Chen, C. Guillaume, Methods and systems for utilizing carbide lime or slag, US 9,902,652 B2, 2018.
- [33] T. Kim, J. Olek, Effects of sample preparation and interpretation of thermogravimetric curves on calcium hydroxide in hydrated pastes and mortars, *Transp. Res. Rec.* 2290 (2012) 10–18. <https://doi.org/10.3141/2290-02>.
- [34] Y. Wang, S. Ramanathan, L. Burris, R.D. Hooton, C.R. Shearer, P. Suraneni, Reactivity of Unconventional Fly Ashes, SCMs, and Fillers: Effects of Sulfates, Carbonates, and Temperature, *Adv. Civ. Eng. Mater.* 11 (2022) 20220003. <https://doi.org/10.1520/acem20220003>.
- [35] R. Bottom, Thermogravimetric Analysis, *Princ. Appl. Therm. Anal.* (2008) 87–118. <https://doi.org/10.1002/9780470697702.ch3>.
- [36] K. De Weerd, K.O. Kjellsen, E. Sellevold, H. Justnes, Synergy between fly ash and limestone powder in ternary cements, *Cem. Concr. Compos.* 33 (2011) 30–38. <https://doi.org/10.1016/j.cemconcomp.2010.09.006>.
- [37] M. Antoni, J. Rossen, F. Martirena, K. Scrivener, Cement substitution by a combination of metakaolin and limestone, *Cem. Concr. Res.* 42 (2012) 1579–1589. <https://doi.org/10.1016/j.cemconres.2012.09.006>.
- [38] A. Arora, G. Sant, N. Neithalath, Ternary blends containing slag and interground/blended limestone: Hydration, strength, and pore structure, *Constr. Build. Mater.* 102 (2016) 113–124. <https://doi.org/10.1016/j.conbuildmat.2015.10.179>.
- [39] F. Deschner, F. Winnefeld, B. Lothenbach, S. Seufert, P. Schwesig, S. Dittrich, F. Goetz-Neunhoeffler, J. Neubauer, Hydration of Portland cement with high replacement by siliceous fly ash, *Cem. Concr. Res.* 42 (2012) 1389–1400. <https://doi.org/10.1016/j.cemconres.2012.06.009>.
- [40] S. Ramanathan, M. Croly, P. Suraneni, Comparison of the effects that supplementary cementitious materials replacement levels have on cementitious paste properties, *Cem. Concr. Compos.* 112 (2020) 103678. <https://doi.org/10.1016/j.cemconcomp.2020.103678>.
- [41] S. Kucharczyk, M. Zajac, C. Stabler, R.M. Thomsen, M. Ben Haha, J. Skibsted, J. Deja, Structure and reactivity of synthetic CaO-Al₂O₃-SiO₂ glasses, *Cem. Concr. Res.* 120 (2019) 77–91. <https://doi.org/10.1016/j.cemconres.2019.03.004>.
- [42] D.P. Bentz, T. Barrett, I. De la Varga, W.J. Weiss, Relating compressive strength to heat release in mortars, *Adv. Civ. Eng. Mater.* 1 (2012) 20120002. <https://doi.org/10.1520/acem20120002>.
- [43] T. Baran, P. Pichniarczyk, Correlation factor between heat of hydration and compressive strength of common cement, *Constr. Build. Mater.* 150 (2017) 321–332. <https://doi.org/10.1016/j.conbuildmat.2017.06.025>.
- [44] K. Scrivener, A. Favier, Investigation of Ternary Mixes Made of Clinker Limestone and Slag or Metakaolin: Importance of Reactive Alumina and Silica Content, *RILEM Bookseries*. (2015) 545–546. <https://doi.org/10.1007/978-94-017-9939-3>.
- [45] F. Georget, B. Lothenbach, W. Wilson, F. Zunino, K.L. Scrivener, Stability of hemihydrate under cement paste-like conditions, *Cem. Concr. Res.* 153 (2022) 106692. <https://doi.org/10.1016/j.cemconres.2021.106692>.